INTERNATIONAL JOURNAL FOR NUMERICAL METHODS IN FLUIDS
Int. J. Numer. Meth. Fluids 2000; **33**: 627–640

Non-linear analysis of solid propellant burning rate behavior

Junye Wang*

College of Mechanical and Electrical Engineering, Zhejiang University of Technology, Hanzhou 310032, China

SUMMARY

The parametric analysis of the thermal wave model of the non-steady combustion of solid propellants is carried out under a sudden compression. First, to observe non-linear effects, solutions are obtained using a computer under prescribed pressure variations. Then, the effects of rearranging the spatial mesh, additional points, and the time step on numerical solutions are evaluated. Finally, the behavior of the thermal wave combustion model is examined under large heat releases (H) and a dynamic factor (β). The numerical predictions show that (1) the effect of a dynamic factor (β), related to the magnitude of dp/dt, on the peak burning rate increases as the value of β increases. However, unsteady burning rate 'runaway' does not appear and will return asymptotically to ap^n, when $\beta \geq 10.0$. The burning rate 'runaway' is a numerical difficulty, not a solution to the models. (2) At constant β and m, the amplitude of the burning rate increases with increasing H. However, the increase in the burning rate amplitude is stepwise, and there is no apparent intrinsic instability limit. A damped oscillation of burning rate occurs when the value of H is less. However, when $H > 1.0$, the state of an intrinsically unstable model is composed of repeated, amplitude spikes, i.e. an undamped oscillation occurs. (3) The effect of the time step on the peak burning rate increases as H increases. Copyright © 2000 John Wiley & Sons, Ltd.

KEY WORDS: combustion instability; combustion model; non-steady combustion; solid propellant

1. INTRODUCTION

In solid rocket propulsion systems, the transient burning rate of a solid propellant under an abrupt changing non-steady pressure condition departs greatly from the steady state burning rate measured in strand-burner experiments. This means that, under transient conditions, the instantaneous pressure level does not dictate the magnitude of the regression rate of a solid propellant.

The ability to predict the burning rate of a solid propellant is of primary importance in the design of high performance solid rocket motors because both the thrust level and the burning time depend upon the burning rate of the propellant. Any improper treatment of the dynamic burning phenomena may cause a significant amount of inaccuracy in predictions of system performance, especially during ignition, extinction by depressurization and resonant burning.

Several models [1–5] have been constructed based on the quasi-steady flame assumption. 'Quasi-steady state of the gas phase' means that the gas phase region should respond and adjust to pressure changes at least an order of magnitude faster than the solid phase thermal

* Correspondence to: Department of Chemical and Process Engineering, The University of Sheffield, Sheffield S1 3JD, U.K.

Received April 1998
Revised December 1998

wave. A main difference in these models can be traced to the method of evaluating the heat feedback from the gas phase flame to the interface or establishing the gradient boundary conditions. In general, these models have been somewhat successful in correlating experimental data after the fact, but are not sufficiently accurate or complete to predict burning rate behavior *a priori*. The majority of these studies put emphasis on describing the heat feedback process and the effects of flame region on solutions. The stability or availability of numerical solutions have yet to be fully examined. Kooker and Nelson [6], indicated that 'Given the major assumption of a quasi-steady flame region, all three combustion models predict nearly the same burning rate response, regardless of the differences in the analysis of the gas phase flame zone. The dominant influence is the response of the thermal wave in the unburned solid.' In this paper it was thought that the boundary condition reconstruction was unnecessary, although it was also important to solutions, and emphasis has been put on the general behaviors of solution of the thermal wave model. A typical model by Krier *et al*. [1] considered the combustion problem on a sufficiently broad scale for large heat evolution or pressurization rate. In that work, an unrealistic result was obtained. The response of propellant burning rate was intrinsically unstable under dynamic conditions with a large heat evolution at the surface or a high pressurization rate even though a steady state solution exists. Kooker's study [6] indicated that the final state of an intrinsically unstable model at constant pressure was composed of repeating finite amplitude spikes, and burning rate 'runaway' was a numerical difficulty and was not a solution to the models during a large heat evolution. A recent study [7] has shown that when a higher pressurization rate, $\beta \geq 10.0$, burning rate 'runaway' does not appear and returns to ap^n after the initial perturbation. Hence, theoretical analysis has yet to be accomplished, such as the influence of non-linearity and the parameter effect.

The objective of the present study is to examine the thermal wave combustion theories originally developed for the study of combustion instability and/or extinguishment in solid propellant rocket motors and to investigate the behavior of the KTSS model by Krier *et al*. Another objective is to see if the desired solution is independent of the techniques used to obtain it. A prescribed time-dependent pressure is simply imposed at the edge of the flame zone. This was done to create a more controlled numerical experimental, though it is physically unrealistic. In keeping with the need for comparative tractability, a preliminary numerical technique is used.

2. MATHEMATICAL MODEL

2.1. Basic equations of the combustion model

In a similar fashion to the previous approaches, the one-dimensional problem is considered and the propellant is homogeneous, incompressible and inert. The region of solid phase reaction is assumed to be sufficiently narrow and close to the solid–gas interface to be considered for surface reactions, i.e. the solid is converted into gas by a global pyrolysis reaction, which occurs at an infinite thin interface. The gas phase flame is quasi-steady and remains anchored to the interface.

As shown schematically in Figure 1, the origin is fixed to the solid–gas interface; therefore, the solid is translating at a velocity equal to the pyrolysis rate $r(t)$. The combustion model reduces to the following initial/boundary value problem describing the thermal wave in the unburned solid propellant (a detailed derivation can be found in [1]):

The energy equation for the solid phase

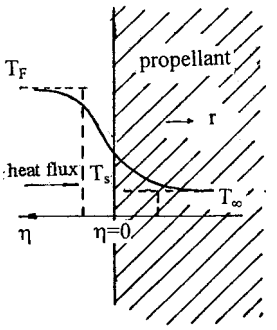

Figure 1. Combustion model configuration.

$$\theta_\tau + R\theta_\eta - \theta_{\eta\eta} = 0. \tag{1}$$

The boundary condition

$$\theta(-\infty, \tau) = 0, \tag{2}$$

$$\theta_\eta(0, \tau) = RH + [P^{2n}(P^{n/m} - H)]/R. \tag{3}$$

The initial condition

$$\theta(\eta, 0) = \mathrm{e}^n. \tag{4}$$

The pyrolysis rate at the surface ($x = 0$)

$$R = \theta_s^m, \tag{5}$$

$$R = P^{n_s} \exp\left[\frac{A(\theta_s - 1)}{1 + (A/E)(\theta_s - 1)}\right]. \tag{6}$$

The pressure function

$$P = 1 + \Delta P(1 - \mathrm{e}^{-\beta\tau}). \tag{7}$$

The response of the solid–propellant combustion to the dynamic pressure functions $P(t)$ is given by the burning rate R, the surface temperature θ_s. Since Equation (5) is simplified from the usual Arrhenius law, $r = A\,\mathrm{e}^{-E_s/\Re T_s}$. In order to evaluate the simplicity and achieve generality, a computational comparison is performed by employing an unsteady Arrhenius expression, Equation (6). For all computations shown in the present paper, $n_s = 0$. Similar to Krier [1], Kooker [6] and Wang [7] also predict a value of burning rate identical to ap^n when the pressure is held constant and the transient portion of the solution has vanished.

The problem is non-linear due to the relation with Equations (1) and (3). An exact analytical solution of the partial differential equation (1) with the foregoing non-linear auxiliary conditions seems improbable. However, numerical solutions are achieved with a digital computer.

2.2. Finite difference equations

Because of the potential difficulty introduced by the non-linearity, the present study examines numerical solution techniques that have been used in previous investigations to solve combustion problems of this type. Numerical experimentation is performed by varying only three parameters for the pressure forcing function considered.

The numerical technique is expressed in the following notation. The superscripts n and $n+1$ refer to the current time level (when the solution is known) and the new time level, respectively. The subscripts $j-1$, j and $j+1$ refer to an arbitrary interior mesh point, j, and its two adjacent neighbors. For reasons to be discussed below, the mesh point distribution is non-uniform and hence $\Delta\eta_{j-1}$, $\Delta\eta_j$ and $\Delta\eta_{j+1}$ are not necessarily equal. The partial differential equation is discretized as follows:

$$\frac{\theta_j^{n+1}-\theta_j^n}{\Delta\tau}+R\frac{\Delta\eta_j^2(\theta_{j+1}^{n+1}-\theta_j^{n+1})-\Delta\eta_{j+1}^2(\theta_j^{n+1}-\theta_{j-1}^2)}{\Delta\eta_j\Delta\eta_{j+1}(\Delta\eta_j+\Delta\eta_{j+1})}$$
$$-2\frac{\Delta\eta_{j+1}(\theta_{j-1}^{n+1}-\theta_j^{n+1})+\Delta\eta_j(\theta_{j+1}^{n+1}-\theta_j^{n+1})}{\Delta\eta_j\Delta\eta_{j+1}(\Delta\eta_j+\Delta\eta_{j+1})}=0.$$

The finite difference equation (FDE) is only an approximation to the partial differential equation (PDE). The relationship between the two is based on Taylor series expansions and can be written as

$$\mathrm{FDE}=\mathrm{PDE}-\frac{\Delta\tau}{2}\theta_{\tau\tau}+[R\Delta\eta_j\Delta\eta_{j+1}+2(\Delta\eta_j-\Delta\eta_{j+1})](\theta_{\eta\eta\eta}/6)$$
$$+[R\Delta\eta_j\Delta\eta_{j+1}(\Delta\eta_{j+1}-\Delta\eta_j)-2(\Delta\eta_j^2-\Delta\eta_j\Delta\eta_{j+1}+\Delta\eta_{j+1}^2)](\theta_{\eta\eta\eta\eta}/24).$$

If the spaced mesh points are equal, the above equation reduces to the more familiar form

$$\mathrm{FDE}=\mathrm{PDE}-\frac{\Delta\tau}{2}\theta_{\tau\tau}+(2R\theta_{\eta\eta\eta}-\theta_{\eta\eta\eta\eta})(\Delta\eta^2/12).$$

Hence, the formal order of accuracy is $O(\Delta\tau)$ and $O(\Delta\eta^2)$. Since the present combustion problem involves a thermal profile that may have very steep gradients near the interface, the spatial mesh must be closely spaced in this region otherwise the truncation error will swamp the desired solution. The spatial steps are so chosen as to satisfy the stability criterion. The full region ($-15\le\eta\le0$) is divided into four sections to determine a 231 point system (21 points, $-0.01\le\eta\le0$; 30 points, $-0.10\le\eta\le-0.01$; 50 points, $-2.00\le\eta\le-0.1$; 130 points, $-15\le\eta\le-2$). The finite difference equation, boundary condition and initial temperature profile in the solid are given by

$$-\frac{(R\Delta\eta_{j+1}+2)\Delta\tau}{\Delta\eta_j(\Delta\eta_j+\Delta\eta_{j+1})}\theta_{j-1}^{n+1}+\left[1+\frac{(2+R(\Delta\eta_{j+1}-\Delta\eta_j))\Delta\tau}{\Delta\eta_j\Delta\eta_{j+1}}\right]\theta_j^{n+1}$$
$$+\frac{(R\Delta\eta_j-2)\Delta\tau}{\Delta\eta_{j+1}(\Delta\eta_j+\Delta\eta_{j+1})}\theta_{j+1}^{n+1}=0_j^n,\quad\text{for } 1\le j\le230; \tag{8}$$

the initial temperature profile

$$\theta_j^0=\begin{cases}\exp[-\Delta\eta_A(231-j)] & (211\le j\le230)\\ \exp[-0.01-\Delta\eta_B(210-j)] & (181\le j\le210)\\ \exp[-0.1-\Delta\eta_C(180-j)] & (131\le j\le180)\\ \exp[-2.0-\Delta\eta_D(130-j)] & (2\le j\le130)\end{cases}; \tag{9}$$

the boundary conditions

$$\theta_0^{n+1}=0, \tag{10}$$

$$\theta_{231}^{n+1} - \theta_{230}^{n+1} = \{RH + [P^{2n}(P^{n/m} - H)]/R\}\Delta\eta_A; \tag{11}$$

the pyrolysis rate

$$R = P^n, \tag{12}$$

$$R = \exp\left[\frac{A(\theta_{231}^{n+1} - 1)}{1 + (A/E)(\theta_{231}^{n+1} - 1)}\right], \tag{13}$$

$$R = (\theta_{231}^{n+1})^m; \tag{14}$$

the pressure function

$$P(I\cdot\Delta\tau) = 1 + \Delta P[1 - \exp(-\beta\cdot I\cdot\Delta\tau)] \quad (I \geq 0). \tag{15}$$

3. MATRIX EQUATION

The following variables are defined:

$$A(0) = 0, \qquad B(0) = 1,$$

$$B(231) = 1, \qquad C(231) = -1,$$

$$\theta_0^n = 0,$$

$$\theta_{231}^n = \{RH + [P^{2n}(P^{n/m} - H)]/R\}\Delta\eta_A$$

$$\left.\begin{aligned} A(I) &= \frac{(R\Delta\eta_j - 2)\Delta\tau}{\Delta\eta_{j+1}(\Delta\eta_j + \Delta\eta_{j+1})} \\ B(I) &= I + \frac{[2 + R(\Delta\eta_{j+1} - \Delta\eta_j)]\Delta\tau}{\Delta\eta_j\Delta\eta_{j+1}} \\ C(I) &= -\frac{(R\Delta\eta_{j+1} + 2)\Delta\tau}{\Delta\eta_j(\Delta\eta_j + \Delta\eta_{j+1})} \end{aligned}\right\} \quad (2 \leq I \leq 230).$$

Equations (8)–(15) are rewritten as

$$\begin{bmatrix} B(231) & C(231) & 0 & \cdots & \cdots & 0 & 0 \\ A(230) & B(230) & C(230) & & & & 0 \\ \vdots & & \ddots & & & & \vdots \\ \vdots & & & \ddots & & & \vdots \\ 0 & & & & A(1) & B(1) & C(1) \\ 0 & 0 & \cdots & \cdots & 0 & A(0) & B(0) \end{bmatrix} \begin{bmatrix} \theta_{231}^{n+1} \\ \theta_{230}^{n+1} \\ \vdots \\ \vdots \\ \theta_1^{n+1} \\ \theta_0^{n+1} \end{bmatrix} = \begin{bmatrix} \theta_{231}^n \\ \theta_{230}^n \\ \vdots \\ \vdots \\ \theta_1^n \\ \theta_0^n \end{bmatrix}. \tag{16}$$

The matrix equation (16) is solved for dynamic rate R by using the full implicit difference scheme.

The method of solution proceeds as follows. At any given instant of time, τ, the values of pressure burning rate and surface temperature are evaluated from Equations (12)–(15). With the calculated values of P, R and T_s, the boundary condition (11) is evaluated by assuming, initially as a first approximation, that $R = P^n$. The matrix equation (16) is solved for temperature. This gives the new temperature profile at the next instant of time $\tau + \Delta\tau$. From

this new temperature profile and new value of surface temperature, the burning rate R is evaluated again from Equation (13) or (14). The newly calculated value of R is used to repeat the entire procedure, until no further change is noted between two adjacent R values. Convergence is assumed when the difference between the R at the new time level and the R at the current is less than a specified tolerance (in this study, 10^{-10} using double precision computation). This is an iterative procedure, where Equation (16) along with the pyrolysis rates (13) and (14) are updated cyclically. This completes the calculation for one step and gives the value of the dynamic burning rate R at the instant $\tau + \Delta\tau$. Table I gives the typical value and range of parameters in this analysis.

The numerical computations are based on the pressure profile described by Equation (7), which is not a good representation of a typical pressure time-history; however, it is relevant to most problems if viewed as a large amplitude pressure wave suddenly passing over a propellant grain that is burning at a steady state. For this reason, any results that follow from Equation (15) are of interest to the present analysis. The ΔP value was approximately 2.5 for most of the experiments, and this value is used for the numerical studies of compression effects. Parameters m and n are held constant at 6 and 0.5 respectively. The dimensionless time τ is written as

$$\tau = (r_0^2/\alpha)t = \left(\frac{\rho_s c_s r_0^2}{k_s}\right)t. \tag{17}$$

Substituting the data of Table I into Equation (19) gives

$$\tau = \frac{1.54 \times 1.55 \times 0.75^2}{0.0031}\, t = 433.125t,$$

i.e. per unit dimensionless time equals 2.31 ms. Differentiating Equation (15) with respect to time τ gives

$$\frac{dP}{d\tau} = \Delta P \cdot \beta \cdot \exp(-\beta\tau). \tag{18}$$

Substituting Equation (17) into Equation (18) and noting that $P = p/p_0$ and when $\tau = 0$, Equation (18) can be written as

$$\left(\frac{dp}{dt}\right)_0 = p_0(\Delta P)(\beta \cdot r_0^2/\alpha). \tag{19}$$

Table I. Parameters of solid propellants

Parameter	Value	Range	Unit
H	0.75	0.45–1.044	
m	6		
n	0.5		
ΔP	2.5		
β	1.0	0.5–∞	
E_s	0.0628		MJ mol^{-1}
ρ_s	1.54		g cm^{-3}
C_s	1.55		J g^{-1} K^{-1}
k_s	0.0031		J cm^{-1} s^{-1} K^{-1}
R_0	0.75		cm s^{-1}
T_{s_0}	623		K
T_∞	278		K

When $p_0 = 12$ bar, $\Delta P = 2.5$, $\alpha/r_0^2 = 7.5$ ms, i.e. $\beta = 1.0$ is corresponding to $(\mathrm{d}p/\mathrm{d}t)_0 = 4000$ bar s^{-1}.

4. RESULTS AND DISCUSSION

Calculations of the burning rate to rapid compression transients are shown in Figures 2–9.

Figure 2 shows the effect of a dynamic factor related to the magnitude of $\mathrm{d}p/\mathrm{d}t$ on the dynamic burning rate. When $\beta < 10.0$, the burning rate response is the same as in Figure 10 of Reference [1]. No runaway appears when $\beta \geq 10.0$ and the burning rate returns to the initial value when $\beta = 2$ at a non-dimensional time of approximately 0.6. This result is different from those of Figure 10 in Reference [1]. In that work, the unbounded burning rate predicted for $\beta = 10$ is one of several calculations used as evidence of burning rate runaway, also called 'an unstable burning rate response'. To see if 'runaway' exists under more extreme conditions, the dynamic factor (β) is increased to ∞. Further computations of this case show that the maximum amplitude increases with increasing β, but when $\beta > 50$, the amplitude oscillates around 9.55. Table II gives these maximum amplitudes of burning rate with variations of β. At any β value the solution remains bounded and does not run away to infinity.

Figure 3 shows the predicted dynamic burning rate under identical input conditions like Figure 7 in Reference [8]. Qualitatively, the burning rate response is the same. The value of peak burning rates is less than those predicted by Kooker *et al.*, which can be traced to a larger time step. Further computations show close agreement with variations of the time step, except near the peak of the burning rate as shown in Figure 4. The peak burning rate increases as the time step decreases. The smaller the time step is, the less the effect is. On the other hand, the effect of the time step on the burning rate is very dependent on two parameters, H and β. To achieve a desired accuracy for the two larger parameters, a smaller time step is needed. The

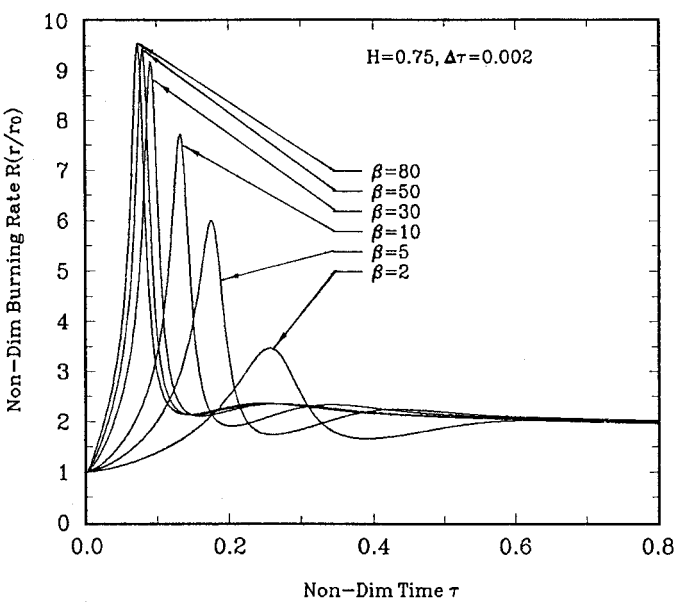

Figure 2. Burning rate response: effect of varying β during compression.

Table II. The maximum values of peak burning rate of propellants with variations of β

Parameter β	Peak burning rate
2	3.548
5	5.99
10	7.73
30	9.17
50	9.47
80	9.54
100	9.57
120	9.55
140	9.56
∞	9.53

$H = 0.75$, $\Delta\tau = 0.002$, $n = 0.5$, $m = 6.0$, $\Delta P = 2.5$

difference of the peak burning rate is of the order of 10% from $\Delta\tau = 0.002$ to $\Delta\tau = 0.00002$ when $\beta = 2.0$. When $\Delta\tau < 0.0015$, the burning rate cures overlap as shown in Figure 4. Table III gives the effects of the time step $\Delta\tau$ on solutions under a fixing H. When H is greater than 0.75, the effect of the time step on the peak burning rate is obvious. Furthermore, the effect increases as H increases. At a larger surface heat release H, this could lead to errors. For example, the peak burning rate is about 30.51 at $\Delta\tau = 0.002$, and the peak burning rate rises to 58.49 at $\Delta\tau = 0.0002$, i.e. the increase of the peak burning rate is 27.98. However, the error will decrease with decreasing the time step. The peak burning rate is 65.24 at $\Delta\tau = 0.0001$, and the peak burning rate rises to 75.44 at $\Delta\tau = 0.00001$. The error decreases from 27.98 to 10.2.

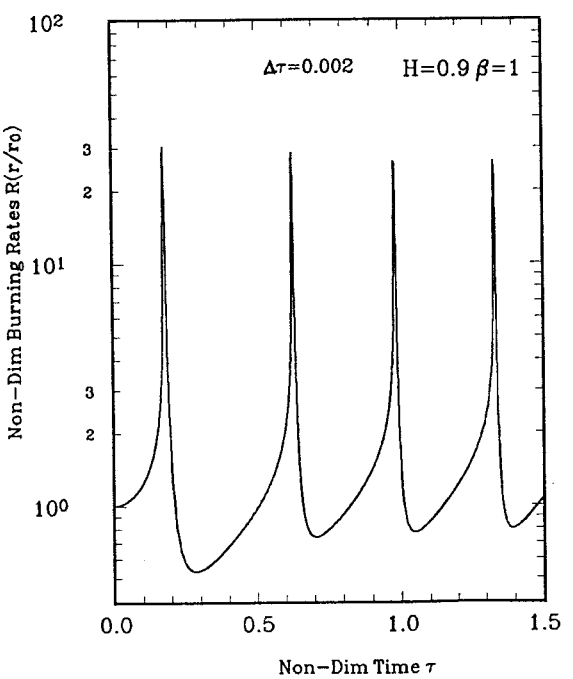

Figure 3. Burning rate response of KTSS model (recomputed results).

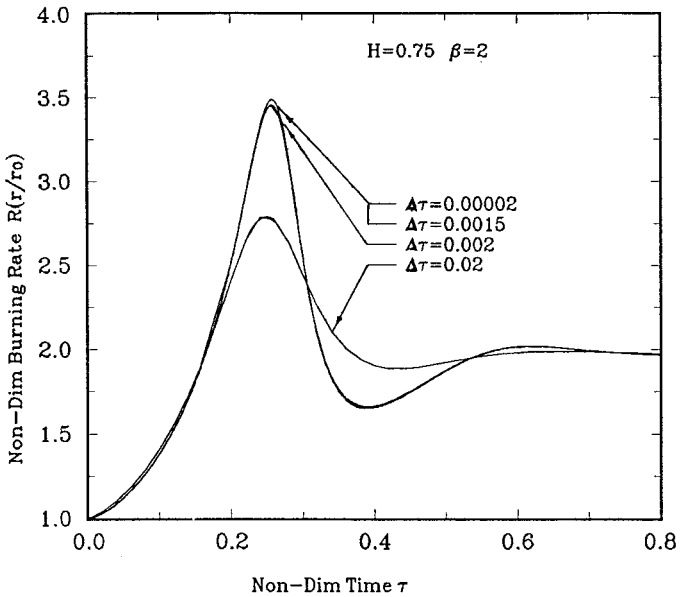

Figure 4. Burning rate response: effect of varying time step during compression.

The larger H is, the less the time step needs to achieve a desired solution. Table IV gives the effects of the time step $\Delta\tau$ on solutions under a fixing β. Hence, the error is not from the method used to obtain it but from a steep gradient burning rate response for a larger H and β. This loss in accuracy can be limited under an acceptable region by selecting a proper time step for any H or β.

On the basis of the computations, a decrease or increase in spatial step yields nearly equal results with acceptable accuracy. Repeating this computation with a 2310 grid point system, which replaces a 231 grid point system, shows that errors of the peak burning rate in Figure 3 are about 10%. When $H = 0.9$ and 1.04, the peak burning rates are 27.39 and 44.68 at $\Delta\tau = 0.002$ respectively. The numerical solution was not sensitive to the spatial step. However, if the spatial step restriction or a sufficient number of mesh points near the propellant interface are eliminated, further computations of this case will predict a divergent solution.

Also of interest is a comparison of between Equation (5) and Equation (6) under identical input conditions when driven by the same exponential pressure profile. Qualitatively, the burning rate response of two equations is the same. However, there occurs a shift of peak burning rate predicted by a power law approximation to the Arrhenius exponential. This is indicated in Figure 5. The shift of the peak burning rate is completely traced to the assumption

Table III. The maximum values of the peak burning rate with changing the time step

β	$\Delta\tau = 0.002$	$\Delta\tau = 0.0002$	$\Delta\tau = 0.00002$
1	2.32	2.348	2.352
2	3.548	3.576	3.589
30	9.17	10.93	11.16

$H = 0.75$, $n = 0.5$, $m = 6.0$, $\Delta P = 2.5$.

Table IV. The first peak burning rate with changing the time step

H	$\Delta\tau = 0.002$	$\Delta\tau = 0.0002$	$\Delta\tau = 0.0001$	$\Delta\tau = 0.00002$	$\Delta\tau = 0.00001$	$\Delta\tau = 0.000005$
0.75	2.32	2.348	2.35	2.352		
0.9	30.51	58.49	65.24	73.86	75.44	76.26
1.0	40.46	86.38	100.3	126.2	132.8	136.8
1.04	44.34	98.29	115.0	148.7	159.7	166.1
1.044	44.36	99.25	113.1	151.1	162.7	169.7

$n = 0.5$, $m = 6.0$, $\Delta P = 2.5$, $\beta = 1.0$.

that $c_p = c_s$ in the computations of the three models [6]. The effect of the pyrolysis rate on the peak burning rate has nearly been considered.

There is considerable interest in the relationship between a possible runaway condition and the intrinsic instability limit of the mathematical model. Figures 6–9 show that as H increases the value of the burning rate amplitude increases. However, the amplitude of the burning rate increases stepwise. There is no apparent intrinsic instability limit. When H is less a damped oscillation occurs, and finally approaches ap^n. When H is larger, an undamped oscillation occurs, which does not approach ap^n. The results shown in Figures 6–9 contain sharp finite amplitude 'spikes', similar to those reported in [6]. An important difference, however, is that the burning rate response in Figures 6–9 is due to a monotonically increasing pressure field and not a uniform pressure field. Although these results appear unconventional, they are the actual solutions to the equations. It is pointed out that the heat release H and the dynamic factor β in the present investigations are probably larger than practical values. However, this

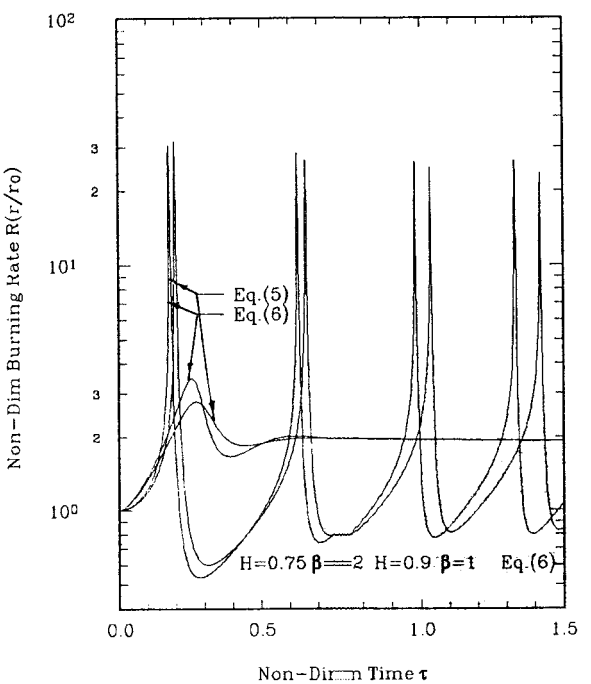

Figure 5. Comparison of burning rate response predicted by two pyrolysis rates at the surface with Equation (5) or (6).

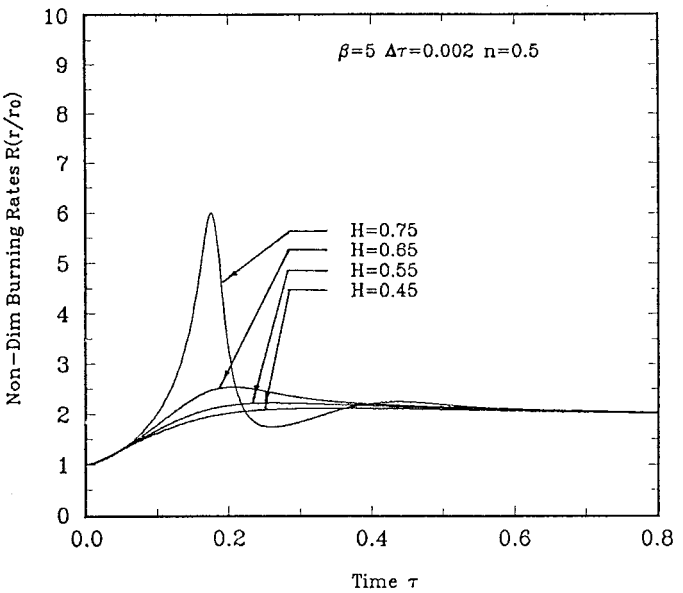

Figure 6. Burning rate response: variation of surface heat release parameter H.

is needed, whether for the development of the thermal wave models or for practical use for the future. The time required for a significant change in burning rate can be obtained from Figures 2–9, as the result of the change in the environment. This change can occur with a small fraction of time α/r_0^2 ($\Delta\tau = 1$), commonly referred to as the characteristic response time of the thermal wave. This time required for change decreases as the value of H or β increases. No

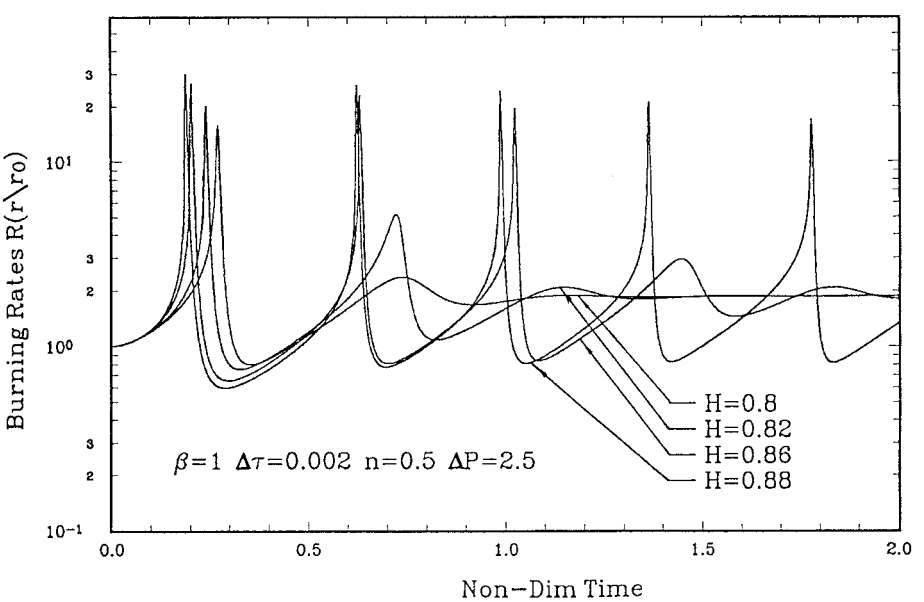

Figure 7. Burning rate response: variation of surface heat release parameter H.

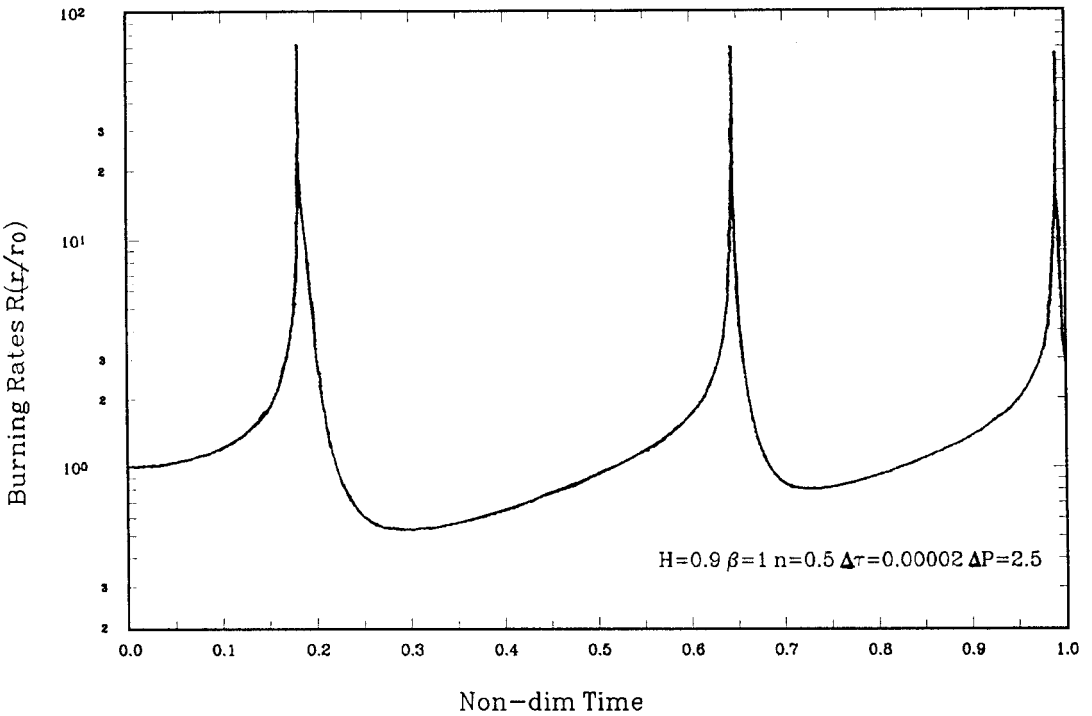

Figure 8. Burning rate response with $H = 0.9$.

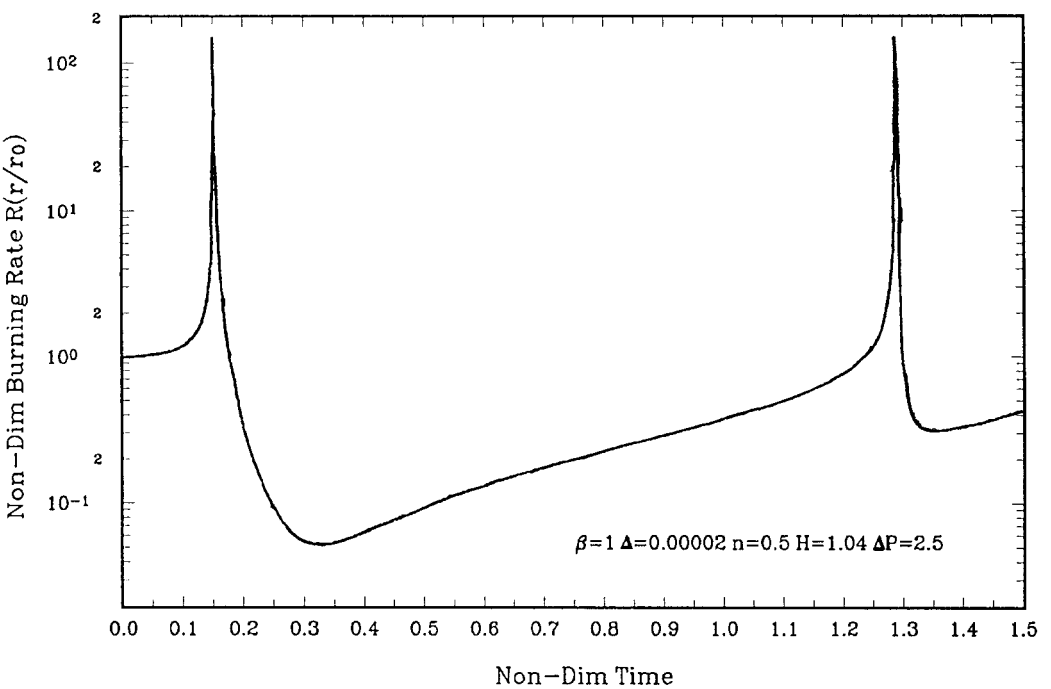

Figure 9. Burning rate response with $H = 1.04$.

directed experimental results can be compared with the predicted dynamic burning rates. However, the effect of pressure change rate on the response time of propellants burning rate measured in [9] is in agreement with the effect of β. In that work, the delay time of the burning rate decreases as the pressure change increases. The experiments underwent a rapid depressurization [10–13], showing that the transient burning rates exhibit low frequency oscillations that are not present in the chamber pressure. Similar to these results, large amplitude spikes may occur, their presence could be obscured by gas phase damping and remain undetected by a wall pressure gage. Hence, the possibility exists that this type of behavior is a triggering mechanism for combustion instabilities.

5. CONCLUSIONS

The effect of a dynamic factor, related to the magnitude of $\mathrm{d}p/\mathrm{d}t$, on the peak burning rate increases as β increases. However, when $\beta > 50$, the peak burning rate does not increase, and the solution remains bounded. The burning rate 'runaway' is a numerical difficulty, and is not a solution to the thermal wave models.

The burning rate amplitude increases with increasing H. However, the increase of the burning rate amplitude is stepwise. There is no apparent intrinsic instability limit. When H is larger, the state of the burning rate is composed of repeated, finite amplitude spikes.

The effect of the time step on the value of peak burning rate increases as the value of H increases. At a greater H, this is not ignored.

The time required for significant changes in burning rate can occur within a time interval smaller than α/r_0^2 ($\Delta\tau = 1$), commonly referred to as the characteristic response time of the thermal wave. This time required for change decreases as the value of H or β increases.

APPENDIX A. NOMENCLATURE

A	$E(1 - T_\infty/T_{s_0})$ (non-dimensional)
c_s	specific heat of solid
c_g	specific heat of gas
E	$E_s/\Re T_{s_0}$ (non-dimensional)
E_s	activation energy of surface reaction
H	$Q_s/c_s(T_{so} - T_\infty)$ (non-dimensional)
k_g	thermal conductivity of gas
k_s	thermal conductivity of solid
m	power of propellant pyrolysis law
n	pressure index in steady burning relation
n_s	pressure index
P	p/p_0 (non-dimensional)
ΔP	amplitude of pressure variation (non-dimensional)
p	pressure
q_g	heat flux of solid–gas interface
Q_s	heat release per unit mass for surface reaction
r	transient burning rate
R	steady burning rate
R	r/r_0 (non-dimensional)

$\Re$	universal gas constant
t	time
T_{s_0}	initial surface temperature
x	dimension

Greek letters

α	$k_s/\rho_s c_s$, thermal diffusivity
β	compression speed parameter
η	$x(r_0/\alpha)$ (non-dimensional)
θ	$(T-T_\infty)/(T_{s_0}-T_\infty)$ (non-dimensional)
ρ_s	density of solid
τ	$t(r_0/\alpha)$ (non-dimensional)

Subscripts

0	initial steady state
j	grid point
η	partial derivative with respect to η

REFERENCES

1. Krier H, T'ien JS, Sirignano WA, Summerfield M. Non-steady burning phenomena of solid propellants: theory and experiments. *AIAA Journal* 1968; **8**: 2200–2207.
2. De Luca L. Non-linear burning stability theory of heterogeneous thin flames. In *18th Symposium (International) on Combustion*. Combustion Institute: Pittsburgh, PA, 1981; 1439–1450.
3. Suhas HK, Bose TK. Non-steady combustion of composite propellants subjected to rapid depressurization. *Combustion Science Technology* 1982; **28**: 55–68.
4. Mongia HC, Ambs LL. A model for the combustion and extinction of composite solid propellants during depressurization. *Combustion and Flame* 1974; **22**: 59–69.
5. Culick FEC. Some recent results for non-linear acoustics in combustion chamber. *AIAA Journal* 1994; **32**: 146–169.
6. Kooker DE, Nelson CW. Numerical solution of solid propellant transient combustion. *ASME Journa of Heat Transfer* 1979; **101**: 359–364.
7. Wang JY, Zhang JX, Sang BC. Effect of rate of pressure change on the combustion of solid propellants. *Acta Armamentarii* 1991; **3**: 84–89 (in Chinese).
8. Kooker DE, Nelson CW. Numerical solution of three solid propellant combustion models during a gun pressure transient. BRL Report No. 1953, USA Ballistic Research Laboratories, Aberdeen Proving Ground, MD, 1977.
9. Wang JY, Sang BC, Wu DD. Experimental studies of transient burning rate delay of composite propellants in response to pressure change. In *Proceedings of the Asian–Pacific Conference on Aerospace Technology and Science*. International Academic Publishers: Beijing, 1994; 893–897.
10. Wang JY, Sang BC. Measurement of transient burning rates of composite propellants in fast depressurization. *Journal of Aerospace Power* 1990; **5**: 173–175 (in Chinese).
11. Yin CF, Hermance CE. Continuous measurement of transient burning rates of composite propellant undergoing rapid depressurization. AIAA Paper 71-173, 1971.
12. Strand LD, Schultz AL, Reedy GK. Microwave Doppler shift technique for determinmg solid propellamt transient regression rates. *Journal of Spacecraft and Rockets* 1974; **11**: 75–83.
13. Wang JY, Sang BC. Laser technique for determining solid propellant transient rates during oscillatory combustion. *Fuels* 1998; **11**(15): 1845–1849.